Depletion forces in fluids

B. Götzelmann, R. Evans,* and S. Dietrich
Fachbereich Physik, Bergische Universität Wuppertal, D-42097 Wuppertal, Federal Republic of Germany
(Received 16 September 1997)

We investigate the entropic depletion force that arises between two big hard spheres of radius R_b, mimicking colloidal particles, immersed in a fluid of small hard spheres of radius R_s. Within the framework of the Derjaguin approximation, which becomes exact as $s=R_s/R_b\to 0$, we examine an exact expression for the depletion force and the corresponding potential for the range $0<h<2R_s$, where h is the separation between the big spheres. These expressions, which depend only on the bulk pressure and the corresponding planar wall-fluid interfacial tension, are valid for all fluid number densities ρ_s. In the limit $\rho_s\to 0$ we recover the results of earlier low density theories. Comparison with recent computer simulations shows that the Derjaguin approximation is not reliable for $s=0.1$ and packing fractions $\eta_s=4\pi\rho_s R_s^3/3\gtrsim 0.3$. We propose two new approximations, one based on treating the fluid as if it were confined to a wedge and the other based on the limit $s=R_s/R_b\to 1$. Both improve upon the Derjaguin approximation for $s=0.1$ and high packing fractions. We discuss the extent to which our results remain valid for more general fluids, e.g., nonadsorbing polymers near colloidal particles, and their implications for fluid-fluid phase separation in a binary hard-sphere mixture. [S1063-651X(98)14405-7]

PACS number(s): 82.70.Dd, 61.20.Gy, 64.75+g

I. INTRODUCTION

Depletion forces arise when two big (colloidal) particles are immersed in a fluid of small colloidal particles, nonadsorbing polymers, micelles, or in a simple fluid. When the separation between the big particles is less than the diameter of the small ones the latter are expelled from the gap between the bigger ones, i.e., there is depletion that leads to an anisotropy of the local pressure, which, in turn, may give rise to an attractive depletion force between the big particles. Such a mechanism was described first by Asakura and Oosawa [1], who suggested that the depletion force could lead to reversible flocculation and phase separation in colloid-polymer mixtures. Those authors calculated the force between two big hard spheres of radius R_b immersed in a fluid of small hard spheres of radius R_s using excluded volume arguments. Their celebrated result [cf. Eq. (2.11)], which is correct to first order in the number density ρ_s of the small component, predicts that the force and the corresponding depletion potential are attractive for all separations $h<2R_s$ and are zero for $h>2R_s$. The physical origin of the attraction is that the exclusion volumes for the small spheres, centered on each big sphere, overlap when $h<2R_s$, increasing the volume that is accessible to the small ones, thereby allowing their entropy to increase. The result is a force that favors the clustering of the big particles and thus provides a possible mechanism for phase separation. Such depletion (or entropic) forces are the focus of much current attention, not just because of their practical importance for understanding the properties of colloid-polymer mixtures [2] but also from a fundamental statistical mechanics viewpoint. That purely entropic effects—all the interparticle forces in the above model are hard-sphere-like—can result in attraction is quite remarkable and has prompted several detailed investigations. Attard and co-workers [3,4] have developed sophisticated hypernetted-chain–based approximations, which include approximate solvent-solvent, solute-solvent, and solvent-solvent bridge diagrams, and tested these in recent Monte Carlo simulations [5] of the depletion force for size ratios $s=0.1$ and 0.2. The integral equation theory appears to be rather accurate for all the packing fractions, $\eta_s=4\pi\rho_s R_s^3/3$ up to 0.34, that were investigated. In an alternative approach to the problem Mao *et al.* [6] have calculated the first three terms in the virial expansion of the force, i.e., up to third order in ρ_s, having first made the Derjaguin approximation in order to relate the force between two particles with large radii of curvature to the force that arises when two small particles are confined by planar walls ($R_b=\infty$). Comparison of their results with molecular dynamics simulations [7] for $s=0.1$ suggests that this third-order approximation performs well, at least for the important range of separations $h\lesssim 2R_s$, even for a packing fraction as high as $\eta_s=0.367$. Note that results from theory and simulation show that although the depletion *potential* remains attractive at contact ($h=0$) this potential becomes repulsive at larger h, with a maximum at $h/(2R_s)=0.7$, as η_s is increased; for $\eta_s\gtrsim 0.2$ the position of this maximum hardly varies as a function of η_s. Such behavior, which is not captured by the Asakura-Oosawa formula valid at low densities, has implications for the possible existence of fluid-fluid phase separations in binary hard-sphere mixtures [7].

Motivated in part by these recent studies we reexamine the theory of depletion forces, focusing for the most part on big hard spheres immersed in a fluid of small hard spheres. Our aim is to construct approximations for the depletion force and the depletion potential that are analytically tractable and that provide some new physical insight into the origin of attraction and repulsion but that go beyond the third-order virial expansion of Mao *et al.* [6]. The starting point is an exact expression for the force between a hard

*Permanent address: H.H. Wills Physics Laboratory, University of Bristol, Bristol BS81TL, United Kingdom.

sphere and a second obstacle immersed in an arbitrary fluid of small particles. Different approximations for the density profile of the fluid at contact with the sphere lead to different approximations for this force.

The paper is arranged such that in Sec. II we describe the exact expression for the depletion force and how the Asakura-Oosawa result emerges as the low density (ideal gas) approximation for the density profile of the fluid at contact. The well-known Derjaguin approximation for the force [cf. Eq. (2.21)] follows by approximating the contact density by that of the fluid in a planar hard wall. By confining the fluid to a wedge rather than a slit, an approximation, cf. Eq. (2.26), is derived that should be more appropriate for large size ratios s. Section III compares the depletion potentials obtained from the approximations of Sec. II with the simulation studies mentioned above. The most significant conclusion is that the Derjaguin approximation provides a poor account of the simulation data for large values of η_s and the size ratios $s=0.1$ and $s=0.2$ employed in the simulations. We discuss the convergence of the virial expansion of the depletion force and conclude that the apparent success of the third-order theory of Ref. [6] may be fortuitous. In Sec. IV we enquire how the depletion potential depends on the choice of interparticle potential functions, i.e., to what extent our results carry over to more general fluids. Section V considers the limit $R_b=R_s$ $(s=1)$, where exact results can be derived. These prompt a new approximation for the depletion potential [cf., Eq. (5.12)], which is shown to be quite successful even for $s=0.1$. Section VI is more speculative and discursive than the earlier sections. It discusses possible repercussions of our results for the structure and the thermodynamic properties of bulk binary mixtures of hard spheres, i.e., for nonzero concentrations of the big spheres. We conclude in Sec. VII with a summary of the results and some discussion of their relevance for experiments that probe depletion forces in colloid-polymer systems.

II. FORCE ON A LARGE FIXED HARD SPHERE

We consider a fluid consisting of small particles of radius R_s in the presence of an external potential $V(\mathbf{R})$ composed of two contributions:

$$V(\mathbf{R};h)=V_1(\mathbf{R})+V_2[\mathbf{R}-(2R_b+h)\mathbf{e}_z], \quad h>0, \tag{2.1}$$

where

$$V_2(\mathbf{R})=\begin{cases}\infty, & R<R_b+R_s\\ 0, & R>R_b+R_s.\end{cases} \tag{2.2}$$

The second term in Eq. (2.1) is the potential due to a big hard sphere of radius R_b (denoted as 2 in Fig. 1 and later in the text) fixed at the position $\mathbf{R}=(x,y,z)=(0,0,2R_b+h)$; $\mathbf{e}_z$ is a unit vector in the z direction. We are particularly interested in the case $R_b>R_s$. The potential $V_1(\mathbf{R})$ can represent any other fixed obstacle, such as another big hard sphere located at the origin [$V_1(\mathbf{R})=V_2(\mathbf{R})$, case (a)] or, e.g., a planar hard wall located a distance h apart from sphere 2 [case (b)]. h is the minimal distance between the two big spheres or between the big sphere and the wall (Fig. 1). We are concerned with

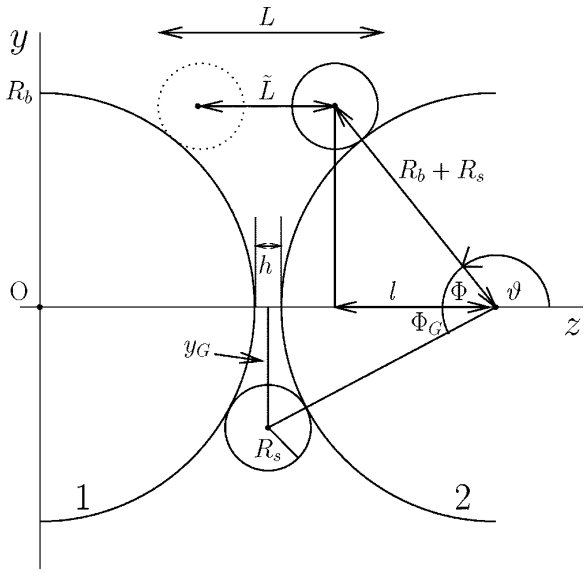

FIG. 1. Two fixed hard spheres of radius R_b, denoted as 1 and 2, in a fluid of smaller hard spheres of radius R_s, drawn for a size ratio $s=R_s/R_b=0.2$. $h\geqslant 0$ measures the minimal distance between the two fixed hard spheres along the z axis connecting the centers $(x,y,z)=(0,0,0)$ and $(0,0,2R_b+h)$. The figure depicts a configuration in which all centers of spheres are located in the plane $x=0$. Φ_G denotes the angle formed when a small hard sphere touches both fixed big hard spheres. ϑ is the angle formed between the z axis and the axis connecting the center of sphere 2 and the center of a small sphere touching sphere 2. $\Phi=\pi-\vartheta$, $l=(R_b+R_s)\cos\Phi$, $y_G=(R_b+R_s)\sin\Phi_G$, $\tilde{L}=2(R_b-l)+h$, and $L=\tilde{L}+2R_s$.

the force $\mathbf{F}(h)$ exerted by the fluid on the big sphere 2. For a general obstacle V_1 its z component is

$$F_z(h)=-\left(\frac{\partial\Omega}{\partial h}\right)_{T,\mu}, \tag{2.3}$$

where Ω is the grand canonical potential of the inhomogeneous fluid in contact with a reservoir at a fixed chemical potential μ and temperature T. A negative value of $F_z(h)$ corresponds to a force directed to the left (Fig. 1). This implies attraction as the grand potential is lowered ($\Delta\Omega<0$) when the sphere is moved to the left towards the obstacle 1 ($\Delta h<0$).

In the Appendix we use density functional methods to derive the following result for the force in terms of the equilibrium number density profile $\rho(\mathbf{R})$ of the fluid:

$$\beta F_z(h)=\int d^3R\,\delta(|\mathbf{R}|-(R_b+R_s))(-z/R) \times\rho(\mathbf{R}+(2R_b+h)\mathbf{e}_z) \tag{2.4}$$

with $\beta=(k_bT)^{-1}$. Although the external potential V_1 does not appear explicitly in this formula, the form of $\rho(\mathbf{R})$ depends on it. The force can also be expressed as

$$\beta\mathbf{F}(h)=-\int_S dA\,\rho(\mathbf{R})\hat{\mathbf{n}}, \tag{2.5}$$

where the integral is over the surface S of a sphere of radius R_b+R_s centered at the center of sphere 2; $\hat{\mathbf{n}}$ is the unit normal vector pointing outwards from this sphere. Equation (2.5) was first derived by Attard [3] directly from the partition function for a hard sphere fluid containing two big hard spheres and was employed in recent Monte Carlo simulations [5] of the force for the particular case of hard spheres. Our present derivation (see the Appendix) emphasizes, first, that this formula is valid for any fluid, not only for one that is composed of (small) hard spheres (the generalization to other fluids is discussed in Sec. IV), and, second, that it remains valid even when an *approximate* density functional is used to obtain the equilibrium density profile. Moreover, Eq. (2.5) holds for any external potential $V_1(\mathbf{R})$, i.e., the obstacle 1 can have various shapes and can exert an arbitrary potential, not necessarily a hard one, on the fluid. In the absence of an external potential ($V_1 \equiv 0$) the density profile has radial symmetry and the net force vanishes. It is the reduction of symmetry induced by the presence of the obstacle at the origin that lends shape to the contact density $\rho(\mathbf{R})$ in Eqs. (2.4) and (2.5) and that gives rise to a nonzero force $F_z(h)$. One can interpret $k_BT\rho(\mathbf{R})$ as a local, kinetic pressure and for a hard sphere the net force is simply a surface integral of this kinetic pressure.

If the potential $V_1(\mathbf{R})$ is radially symmetric around the z axis, as in the cases (a) and (b), the density profile has the same symmetry and Eqs. (2.4) and (2.5) lead to [5]

$$\beta F_z(h) = -2\pi(R_b+R_s)^2 \int_0^\pi d\vartheta \sin\vartheta\cos\vartheta\,\rho(\vartheta), \tag{2.6}$$

where $\rho(\vartheta)$ is the contact density of the small hard-sphere fluid at the fixed big sphere 2 and ϑ is the angle between the z axis and the axis connecting the center of sphere 2 and the center of a small sphere touching the large one (see Fig. 1). In this case $F_x = F_y = 0$. Equation (2.6) can be reformulated as

$$\beta F_z(h) = 2\pi(R_b+R_s)^2 \int_{\pi/2}^\pi d\vartheta \sin\vartheta(-\cos\vartheta)\Delta\rho(\vartheta). \tag{2.7}$$

Here $\Delta\rho(\vartheta) = \rho(\vartheta) - \rho(\pi-\vartheta)$, with $\pi/2 < \vartheta < \pi$, is the difference of the contact densities between the left $[\rho(\vartheta)]$ and the right $[\rho(\pi-\vartheta)]$ hemisphere of sphere 2. For a fixed value of the y coordinate $\tilde{L}$ denotes the distance in the z direction a small sphere can move until it touches one of the two surfaces of the obstacles. In case (a), corresponding to two big spheres, one has $\tilde{L} = 2R_b + h - 2l$ (see Fig. 1) and in case (b), corresponding to a big sphere a distance h in front of a planar wall, $\tilde{L} = R_b + h - l - R_s$ with $l = -(R_b + R_s)\cos\vartheta > 0$. Note that with these definitions one has $\tilde{L} = h - 2R_s$ for $\vartheta = \pi$ and $\tilde{L} = h + 2R_b$ for $\vartheta = \pi/2$ for case (a). Changing variables from ϑ to $\tilde{L}$ and defining $L \equiv \tilde{L} + 2R_s$ (see Fig. 1) we obtain the *exact* equation

$$\beta F_z(h) = \pi\epsilon \int_h^\infty dL[(R_b+R_s) - \tfrac{1}{2}\epsilon(L-h)]\Delta\rho(L), \tag{2.8}$$

where $\epsilon = 1$ for the sphere-sphere case [case (a)] and $\epsilon = 2$ for the sphere-wall case [case (b)]. $\Delta\rho(L)$ denotes the difference of the contact densities between the left and right hemisphere of sphere 2 and is defined to be zero for $L > (2/\epsilon)(R_b+R_s) + h$. It depends also on the choice of the geometry, i.e., on ϵ and on the radii of the spheres. For small size ratios $s \equiv R_s/R_b \ll 1$ this additional dependence is expected to be rather weak but, in general, this dependence can be significant.

The calculation of the density profile $\rho(\mathbf{R})$ at contact, either by simulation or by minimizing a suitable density functional, requires considerable numerical effort so that it is important to develop approximation schemes for $\rho(\mathbf{R})$. These can provide physical insight into the factors that lead to an entropic attraction or repulsion. To this end Eq. (2.8) is a convenient starting point. If one assumes that $\Delta\rho(L)$ decays rapidly as a function of L over the range of the integration, the second integral in Eq. (2.8) should be negligible so that one finds

$$\beta F_p(h) = \pi\epsilon(R_b+R_s) \int_h^\infty dL\,\Delta\rho(L). \tag{2.9}$$

We refer to this approximation as the projection approximation since it corresponds to ignoring the factor $(-z/R)$ in Eq. (2.4) and the factor $\cos\vartheta$ in Eq. (2.7), respectively. Thus the projection approximation disregards the projection onto the z axis that appears in the exact formula. Equation (2.9) already indicates that to leading order in R_b the force should depend linearly on the radius R_b. Moreover, it is reasonable to expect that for a given value of R_b the contact density difference $\Delta\rho(L)$ is almost the same for case (a) and case (b). (This should be true for intermediate as well as small size ratios s.) With this additional approximation Eq. (2.9) implies that the force-separation curves for the two cases should differ by a factor of approximately 2. Direct support for this prediction is provided by the Monte Carlo results (see Fig. 8 in Ref. [5]) of Dickman *et al.* for a size ratio $s \equiv R_s/R_b = 0.1$. Note that in Ref. [5] the authors argue that the comparison of the results of case (a) with those of case (b) amounts to a test of the Derjaguin approximation. However, we emphasize that the Derjaguin approximation involves further assumptions, namely, that $\Delta\rho(L)$ should be replaced by the corresponding quantity for a planar slit (see Sec. II B). The Derjaguin approximation does, of course, lead to a factor of precisely 2 for the ratio of forces but Eq. (2.9) indicates that a factor of approximately 2 should follow from less drastic assumptions and therefore should hold for a wider class of approximations. It is sufficient that $\Delta\rho(L)$ for two macrospheres and for a wall and a macrosphere are similar. Therefore the appearance of this factor of 2 is a necessary but not sufficient criterion for the validity of the Derjaguin approximation.

Another approximation scheme consists of calculating the density profiles for two separated systems, where in the first one only V_1 is considered and in the second one only V_2. One then superposes the two density profiles of the two isolated systems in order to obtain an estimate of the density profile of the combined system [3]. In the following subsections we describe some other approximate approaches and discuss the relationship between them as well as their impli-

cations for the dependence of the depletion force on the density (volume fraction) of the small spheres.

A. The Asakura-Oosawa approximation and an extension

If one assumes that the density profile is not disturbed by the presence of the external potential until h is so small that no small sphere can be accommodated between the obstacle 1 and the big sphere 2, i.e., the density on a part of the left hemisphere of sphere 2 is zero, the contact density difference is given by

$$\Delta\rho_s(L)=\begin{cases}-\rho_s, & L<2R_s\\ 0, & L>2R_s,\end{cases} \tag{2.10}$$

where ρ_s is the number density of the uniform (bulk) fluid. This approximation is only justified for very low bulk densities for which it should become exact. Inserting Eq. (2.10) into the exact Eq. (2.8) one obtains

$$\beta F_A(h)=-\pi\epsilon\rho_s\Theta(2R_s-h)[R_b+(1-\tfrac{1}{2}\epsilon)R_s+\tfrac{1}{4}\epsilon h]\times(2R_s-h), \tag{2.11}$$

i.e., the force is negative (attractive) for $h<2R_s$ and vanishes for $h>2R_s$. Again, $\epsilon=1$ refers to case (a) and $\epsilon=2$ to case (b) and $\Theta(r)$ denotes the Heaviside step function. Equation (2.11) is the well-known result obtained by Asakura and Oosawa [1] more than 40 years ago using excluded volume arguments. Using Eq. (2.10) in the projection approximation [Eq. (2.9)] one has

$$\beta F_{pA}(h)=-\pi\epsilon\rho_s\Theta(2R_s-h)(R_b+R_s)(2R_s-h), \tag{2.12}$$

which is again negative for $h<2R_s$ and vanishes otherwise. The ratio of the forces given by these two equations is largest at $h=0$:

$$\frac{F_A(0)}{F_{pA}(0)}=\frac{R_b+\left(1-\frac{1}{2}\epsilon\right)R_s}{R_b+R_s}=1-\frac{1}{2}\epsilon\frac{s}{1+s}. \tag{2.13}$$

For $s=0.1$ this ratio is 0.91 for case (b) and 0.95 for case (a). For smaller values of s this ratio approaches 1.

In an attempt to improve this approximation one can allow for the disturbance of the small sphere fluid by the fixed sphere 2 but ignores the influence of the other obstacle, i.e., V_1. For a single hard sphere of radius R_b immersed in a hard-sphere fluid with the bulk density ρ_s, the contact density ρ_c is accurately approximated by [8]

$$\frac{\rho_c(s,\eta_s)}{\rho_s}=\frac{1-\eta_s/2}{(1-\eta_s)^3}+\eta_s\frac{3/2+\eta_s(1-\eta_s)}{(1-\eta_s)^3}\frac{2R_b-2R_s}{2R_b+2R_s}, \tag{2.14}$$

where $\eta_s=(4\pi/3)R_s^3\rho_s$ is the volume fraction of the small spheres. This equation follows from a careful fit to simulation data and in the limit $R_b\to\infty$ it reduces to the result for the contact density at a single planar hard wall $\rho_c(s\to0,\eta_s)=\beta P$ where P is the pressure of the uniform hard-sphere fluid given by the Carnahan-Starling [9] equation of state. Note that for size ratios $s<0.1$ the values obtained from Eq. (2.14) differ only slightly from those in the limit $s=0$. As expected from the equation of state of the ideal gas one has $\rho_c(s,\eta_s\to0)=\rho_s$. Equation (2.10) can be generalized by replacing ρ_s by ρ_c. Within the projection approximation we then obtain

$$\beta F_{pA2}(h)=-\pi\epsilon\rho_c\Theta(2R_s-h)(R_b+R_s)(2R_s-h), \tag{2.15}$$

which constitutes an empirical extension of Eq. (2.12) to larger values of η_s. The quality of this approximation will be discussed in Sec. III B.

B. The Derjaguin approximation

In the case of a small size ratio $s\ll1$, the small spheres between the two big hard spheres are exposed to an external field, which for fixed y (see Fig. 1) can be approximated by that of a planar hard-wall slit of width L. Thus the contact density at the left hemisphere of the fixed sphere 2 is approximated by the contact density $\rho_{\rm slit}(L)$ of a hard sphere fluid confined to a slit of width L. The contact density on the right hemisphere is approximated by that at a single planar wall, i.e., that of a slit of infinite width, $L\to\infty$. Thus the difference in the contact densities is given by $\rho_{\rm slit}(L)-\rho_{\rm slit}(\infty)$ with $\rho_{\rm slit}(\infty)=\beta P(\rho_s)$. From a force sum rule [10,11] this difference is β times the so-called solvation force $f_s(L)$, the excess pressure due to confinement of the fluid, in a slit composed of hard walls. Using this approximation in Eqs. (2.8) and (2.9) leads to

$$F_D(h)=\pi\epsilon\int_h^\infty dL[(R_b+R_s)-\tfrac{1}{2}\epsilon(L-h)]f_s(L) \tag{2.16}$$

and

$$F_{pD}(h)=\pi\epsilon(R_b+R_s)\int_h^\infty dL\,f_s(L), \tag{2.17}$$

respectively. In both Eqs. (2.16) and (2.17) the upper limit of integration is extended to infinity, although strictly speaking this limit should be $L=(2/\epsilon)(R_b+R_s)+h$. However, $f_s(L)$ vanishes sufficiently rapidly that this causes a negligible error [11]. Equation (2.17) is called the Derjaguin approximation [12] because it is equivalent to the general formula obtained by Derjaguin [13] relating the force between convex bodies to the excess free energy of a fluid confined between planar walls. The advantage of Eqs. (2.16) and (2.17) is that the only required input is that from the planar (slit) geometry. This input can be determined more easily, e.g., by density functional theory [11], simulation [14], virial expansions [6], and integral equation closures [15]. A more formal way of defining this approximation is to demand that in Eqs. (2.8) and (2.9) $\Delta\rho(L)$ should not depend on R_b. Then the value for $R_b\to\infty$ can be used, which is $\rho_{\rm slit}(L)-\rho_{\rm slit}(\infty)$, leading directly to Eqs. (2.16) and (2.17). One can argue that Eqs. (2.16) or (2.17) represent the best approximation one can apply without taking explicit account of the dependence of the contact density on the size ratio s.

We now consider Eq. (2.17) for $0<h<2R_s$. For $L<2R_s$ all spheres are squeezed out of the slit so that the contact density is zero and the solvation force is constant and given by minus the bulk pressure of the fluid:

$$f_s(L)=-P(\rho_s), \quad 0<L<2R_s. \tag{2.18}$$

On the other hand, by definition, one has for any slit width

$$f_s(L)\equiv-\frac{1}{A}\left(\frac{\partial\Omega}{\partial L}\right)_{\mu,T}-P(\rho_s)=-\left(\frac{\partial\gamma(\rho_s;L)}{\partial L}\right)_{\mu,T}, \tag{2.19}$$

where $\gamma(\rho_s;L)$ is the finite size contribution to the grand potential per unit area A for a hard-wall slit of width L [11]. If these relations are inserted into Eq. (2.17), one obtains

$$F_{pD}(h)=-\pi\epsilon(R_b+R_s)[P(\rho_s)(2R_s-h)+\gamma(\rho_s;\infty)-\gamma(\rho_s;2R_s)], \quad 0<h<2R_s. \tag{2.20}$$

In Ref. [11] it is shown that $\gamma(\rho_s;2R_s)$ vanishes identically so that

$$F_{pD}(h)=-\pi\epsilon(R_b+R_s)[P(\rho_s)(2R_s-h)+\gamma(\rho_s)], \quad 0<h<2R_s, \tag{2.21}$$

where $\gamma(\rho_s)\equiv\gamma(\rho_s,\infty)$ is twice the wall-fluid interfacial tension of a single wall. Note that $\gamma(\rho_s)$ is *negative* for hard spheres at a hard wall. Equation (2.21) is a formally exact result within the general framework of the Derjaguin approximation. Note that the same formula is given by Attard *et al.* [16]. When $h=2R_s$, so that a small sphere can just bridge the gap between the obstacles, the force simplifies to $\beta F_{pD}(2R_s)=-\pi\epsilon(R_b+R_s)\gamma(\rho_s)$. This last result, which is valid for any fluid, is presented explicitly in Derjaguin's original work [13]. Note that Eq. (2.21) is valid for all fluid densities ρ_s. This is in strong contrast to the Asakura-Oosawa approximation, which is valid only for low densities. Moreover, as the Derjaguin approximation becomes exact in the limit $R_b\to\infty$, Eq. (2.21) is also exact in that limit. Equation (2.21) shows nicely the interplay between attractive and repulsive contributions. The depletion of the small spheres acts to push the big sphere on the right side towards the left by a force that equals the bulk pressure $P(\rho_s)$ times the depleted area $\Delta A(h)$:

$$\Delta A(h)\equiv 2\pi(R_b+R_s)^2\int_0^{\Phi_G}d\Phi\sin\Phi=\pi\epsilon(R_b+R_s)(2R_s-h). \tag{2.22}$$

Here we used the relations $\cos\Phi_G=(R_b+\frac{1}{2}h)/(R_s+R_b)$ (see Fig. 1) in case (a) and $\cos\Phi_G=(R_b+h-R_s)/(R_b+R_s)$ in case (b). This implies that the first term in Eq. (2.21) leads to an attraction that is essentially the same as in Eq. (2.15). On the other hand, the density of the small spheres in the wedge formed by the two big spheres is enlarged [17], leading to repulsion. The overall contribution due to this repulsion is given by the second, surface tension, term, which is independent of h, as the Derjaguin approximation neglects all curvature effects. This repulsive contribution is completely ignored both in the Asakura-Oosawa approximation, Eq. (2.11), and in Eq. (2.15).

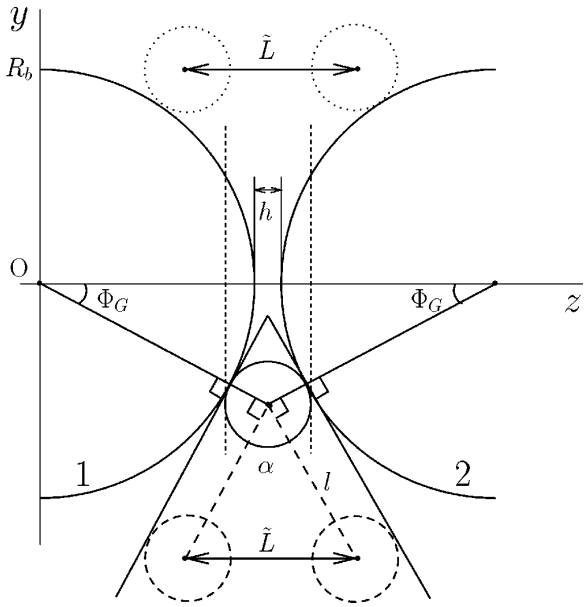

FIG. 2. Introduction of the wedge approximation for the same geometry as in Fig. 1 (see the main text). The wedge with opening angle α is defined such that its sides are perpendicular to the lines connecting the centers of the big spheres and the center of a small sphere, which just touches both big spheres. Thus one has $\cos(\alpha/2)=\cos\Phi_G=(R_b+\frac{1}{2}h)/(R_s+R_b)$.

C. The wedge approximation

The Derjaguin approximation invokes the solvation force $f_s(L)$ for a parallel slit in order to estimate the force between the big spheres. For hard spheres $f_s(L)$ oscillates with a period $\sim 2R_s$ and its envelope decays exponentially. The integral in Eq. (2.17) is dominated by values of $f_s(L)$ for $L\lesssim 3R_s$ or $4R_s$ (see Ref. [18]). In Fig. 2 a single small sphere is shown at a position $\tilde{L}=0$ or $L=2R_s$ for a size ratio $s=0.2$. In order to estimate the values of the density $\rho(\mathbf{R})$ in this case, it seems hardly justified to approximate the system by a slit (see the short-dashed line in Fig. 2). In this case the deviations from planar geometry are very pronounced and the small particles can enter and leave more easily than in a slit. Thus we propose to replace the slit by a wedge of angle $\alpha=2\Phi_G$, i.e., for a given distance $\tilde{L}$ between the centers of the dotted spheres in Fig. 2 we approximate the contact density at the fixed sphere 2 by the contact density in a wedge with hard walls forming a fixed angle α and the same distance $\tilde{L}$ (see the dashed spheres in Fig. 2). Using this approximation in the projection approximation [Eq. (2.9)] for the force acting on sphere 2 we obtain an equation that contains an integration over the contact density $\rho_w(l)$ at one of the sides of a wedge instead over the solvation force of a slit. Thus we define

$$I(\alpha)\equiv\sin\alpha\int_0^\infty dl[\rho_w(l)-\rho_w(\infty)], \tag{2.23}$$

where the factor $\sin\alpha$ has been included in order to yield a

finite value of $I(\alpha)$ for $\alpha=0$. A close investigation of this quantity leads to some exact results and a symmetry property, which can be exploited to determine the first seven coefficients in a Fourier expansion of Eq. (2.23) [19], yielding what should be a very accurate approximation:

$$I(\alpha)=-\frac{\beta}{2}\gamma(\rho_s)(1+\cos\alpha). \tag{2.24}$$

This result is consistent with the exact sum rule $I(\pi/2)=-\beta\gamma(\rho_s)/2$ [20]. [Note that $\gamma(\rho_s)$ is twice the surface tension between the fluid and a *single* wall.] A substitution of variables in Eq. (2.23) gives

$$I(\alpha)=\frac{\sin\alpha}{2\sin(\alpha/2)}\int_{2R_s}^{\infty}dL[(\rho_w(L)-\rho_w(\infty)], \tag{2.25}$$

which facilitates the use of Eq. (2.24) in the projection approximation given by Eq. (2.9) and leads, together with Eq. (2.18), to the wedge approximation

$$F_{pw}(h)=-\pi(R_b+R_s)[P(\rho_s)(2R_s-h)+\gamma(\rho_s)\cos\Phi_G],$$
$$0<h<2R_s, \tag{2.26}$$

with $0\leqslant\cos\Phi_G=(R_b+h/2)/(R_b+R_s)\leqslant 1$. In the limits $s=R_s/R_b\to 0$ and $h/R_b\to 0$ we recover the Derjaguin approximation [Eq. (2.21)]. For $s=\sqrt{2}-1$ and $h=0$, which corresponds to $\alpha=\pi/2$ where the sum rule for $I(\alpha)$ is exact, one has $\cos\Phi_G=1/\sqrt{2}=0.707$. Thus the repulsion between the two fixed spheres is reduced within this new approximation. From this observation we expect that in an exact treatment the repulsion should be diminished further, as even a wedge (see Fig. 2) restricts the small spheres more than the actual configuration.

III. DEPLETION POTENTIAL FOR A HARD SPHERE FLUID

For subsequent applications the potential energy associated with depletion is the important physical quantity. The depletion potential $W(h)$ is the potential energy required to bring a hard sphere of radius R_b from infinity to a distance h from another hard sphere with radius R_b ($\epsilon=1$) or from a hard wall ($\epsilon=2$)

$$W(h)\equiv\int_h^{\infty}dh'F(h'). \tag{3.1}$$

For the remainder of this section we specialize to a hard-sphere fluid and consider the various approximations for the depletion force $F(h)$ that were introduced in Sec. II. Since most of those approximations provide explicit results for $F(h)$ in the range $0\leqslant h\leqslant 2R_s$ it is convenient to focus on the potential difference

$$W(h)-W(2R_s)=\int_h^{2R_s}dh'F(h'). \tag{3.2}$$

Moreover, since the leading dependence of $W(h)$ on the radius R_b is given by a prefactor (R_b+R_s) [see, e.g., Eq. (2.9)], this motivates the following definition of a normalized (dimensionless) potential:

$$\Delta W(h)\equiv\frac{2R_s}{R_b+R_s}\frac{1}{\epsilon}\beta[W(h)-W(2R_s)]. \tag{3.3}$$

A. Asakura-Oosawa depletion potential

Substituting Eq. (2.11) into Eq. (3.1) and integrating leads to the Asakura-Oosawa approximation for the depletion potential,

$$\beta W_A(h)=\begin{cases}-\rho_s\Delta V(h), & h<2R_s\\ 0, & h>2R_s,\end{cases} \tag{3.4}$$

where

$$\Delta V(h)=\pi\epsilon(2R_s-h)\Big\{R_s[R_b+(1-\tfrac{1}{3}\epsilon)R_s]$$
$$-\frac{1}{2}h[R_b+(1-\tfrac{2}{3}\epsilon)R_s]-h^2\tfrac{1}{12}\epsilon\Big\}. \tag{3.5}$$

Note that $\Delta V(h)$, which results here from a straightforward integration of Eq. (2.11), can be identified with the overlap volume of two exclusion spheres of radius R_b+R_s ($\epsilon=1$) or of an exclusion sphere and a hard wall ($\epsilon=2$) (see Fig. 1). For sufficently small size ratios s the projection approximation is accurate and the above equation simplifies considerably, i.e., using Eq. (2.12) in Eq. (3.2) yields

$$\beta W_{pA}(h)=\begin{cases}-\rho_s\dfrac{\pi}{2}\epsilon(R_s+R_b)(2R_s-h)^2, & h<2R_s\\ 0, & h>2R_s.\end{cases} \tag{3.6}$$

Defining the packing fraction $\eta_s=4\pi\rho_s R_s^3/3$ and the dimensionless distance $\lambda=(h-2R_s)/(2R_s)=-1+h/(2R_s)$, the normalized potential is

$$\Delta W_{pA}(\lambda)=\begin{cases}-3\eta_s\lambda^2, & -1<\lambda<0\\ 0, & \lambda>0,\end{cases} \tag{3.7}$$

which, unlike the normalized potential following from Eq. (3.4), is independent of s and ϵ. The Asakura-Oosawa potential is attractive and increases linearly with increasing fluid density ρ_s.

B. Derjaguin depletion potential

Using the Derjaguin approximation [Eq. (2.21)] in Eq. (3.2) leads to

$$W_{pD}(h)-W_{pD}(2R_s)=-\epsilon\pi(R_b+R_s)(2R_s-h)\times\left(\frac{1}{2}P(\rho_s)(2R_s-h)+\gamma(\rho_s)\right),$$

$$0<h<2R_s, \tag{3.8}$$

which is exact in the context of the Derjaguin approximation. The corresponding normalized interaction potential is

$$\Delta W_{pD}(\lambda)=-\pi\left(\frac{1}{2}\tilde{P}(\rho_s)\lambda^2+2\tilde{\gamma}(\rho_s)\lambda\right), \quad -1<\lambda<0, \tag{3.9}$$

where $\tilde{P}\equiv\beta P(\rho_s)(2R_s)^3$ is the reduced pressure and $\tilde{\gamma}=-\beta\gamma(\rho_s)(2R_s)^2/2>0$ is minus the reduced surface tension of a hard sphere liquid close to a *single* hard wall. Note that the normalized interaction potential in Eq. (3.9) is independent of the size ratio $s=R_s/R_b$ and of ϵ; it is the same for the interaction between a wall and a fixed sphere as for two equal fixed spheres. The usefulness of Eqs. (3.8) and (3.9) lies in the fact that highly accurate, analytic formulas for $\tilde{P}$ and $\tilde{\gamma}$ are known. In the following we use the Carnahan-Starling relation for the pressure [9]

$$\tilde{P}(\rho_s)=\frac{6}{\pi}\eta_s\frac{1+\eta_s+\eta_s^2-\eta_s^3}{(1-\eta_s)^3} \tag{3.10}$$

and the scaled particle theory (SPT) [21] for the surface tension

$$\tilde{\gamma}(\rho_s)=\frac{9}{2\pi}\frac{\eta_s^2(1+\eta_s)}{(1-\eta_s)^3}. \tag{3.11}$$

Using more sophisticated results for $\tilde{P}$ and $\tilde{\gamma}$ [22] leads to very similar results for the depletion potential. Moreover, making variations of a few percent from the values of P and γ given by the Carnahan-Starling and scaled particle results does not have a significant effect on the form of the depletion potential.

Much insight is gained by expanding Eq. (3.9) in powers of the packing fraction:

$$\Delta W_{pD}(h)=-3\lambda^2\eta_s+(-9\lambda-12\lambda^2)\eta_s^2+(-36\lambda-30\lambda^2)\eta_s^3-54\lambda(\tfrac{3}{2}+\lambda)\eta_s^4+O(\eta_s^5), \quad -1<\lambda<0. \tag{3.12}$$

At first order in η_s we recover Eq. (3.7), the Asakura-Oosawa result in the projection approximation, which is, therefore, completely contained in Eq. (3.9). This is due to the fact that the surface tension $\tilde{\gamma}$ is, in lowest order, quadratic in η_s. Thus, the first-order term in Eq. (3.12) is given by the first-order (ideal gas) term in the pressure $\tilde{P}$. This is equivalent to the assumption used in the derivation of the Asakura-Oosawa approximation. Note that for the second-order term in Eq. (3.12) the surface tension contribution is *equally* important. Therefore improving only the estimate of $\tilde{P}$, which is equivalent to calculating the contact density ρ_c to higher order in η_s [see Eq. (2.15)], does not constitute a systematic improvement of the Asakura-Oosawa approximation.

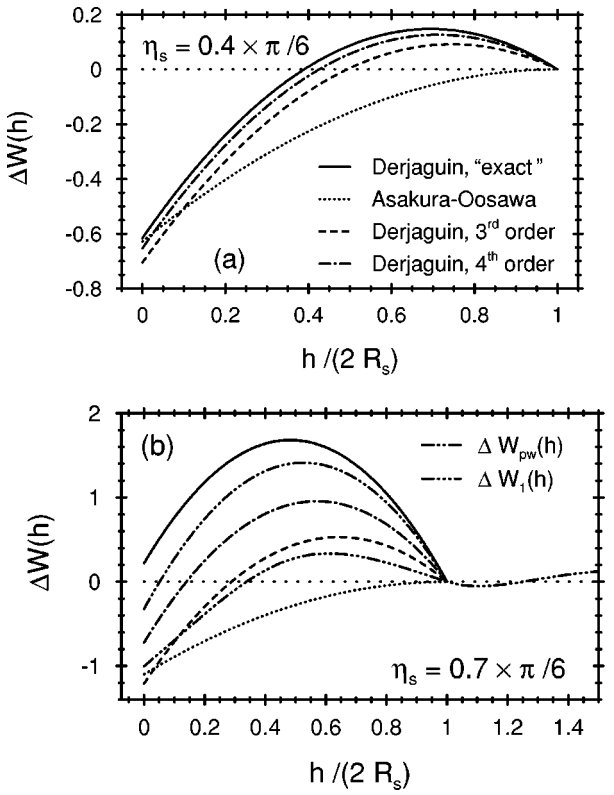

FIG. 3. The normalized depletion potential $\Delta W(h)$ [Eq. (3.3)] for a packing fraction $\eta_s=0.4\times\pi/6=\pi/15=0.2094$ (a) and for $\eta_s=0.7\times\pi/6=0.3665$ (b). In both (a) and (b) the full line denotes the ''exact'' Derjaguin result [Eqs. (3.9)–(3.11)] and the dotted line denotes the Asakura-Oosawa (projection) approximation [Eq. (3.7)]. The dashed and the dashed-dotted lines denote the result up to third and fourth order in η_s, respectively [see Eq. (3.12)]. The third-order result is almost identical to the result obtained in Ref. [6]. In (b) the dashed-double-dotted line denotes the result of the wedge approximation [Eq. (3.15)] for $\epsilon=1$ and with $s=0.2$. The dashed-triple-dotted line corresponds to the result of the limit $R_b=R_s$ [Eq. (5.12)] ($\epsilon=1$). This is the only case for which we show results for $h>2R_s$. By definition $\Delta W(h=2R_s)=0$.

Recently Mao *et al.* [6,23] have developed a virial expansion approach for calculating the depletion potential within the framework of the Derjaguin approximation, i.e., by using the planar (slit) geometry. Within their approach it is possible to calculate the depletion potential exactly up to third order in η_s, for all h. In the range $0<h<2R_s$ our present approach reproduces their result, if one uses formulas for $\tilde{P}$ [22] and $\tilde{\gamma}$ [24] that yield the exact virial coefficients up to third order. In order to obtain a simple expansion we use approximations, given by Eqs. (3.10) and (3.11), which yield the exact first two virial coefficients. However, a comparison with the results in Ref. [6] shows that the differences at third order are at most a few percent. We emphasize that Eqs. (3.10) and (3.11) are known to be accurate to all orders of η_s not just to third order.

In Fig. 3(a) the normalized depletion potential obtained from Eq. (3.9) is shown as a function of $h/(2R_s)$ for $\eta_s=0.2094$. Even at this fairly low packing fraction the first-

order, Asakura-Oosawa, approximation is very inaccurate. It is only useful for very small packing fractions. The third-order result yields a shape similar to the ''exact'' result (i.e., without expansion) but even the fourth-order result shows significant deviations from the ''exact'' one. It is necessary to include fifth-order terms in order to obtain a satisfactory agreement with the ''exact'' result. For a higher packing fraction, $\eta_s = 0.3665$, the third-order result is even qualitatively incorrect [see Fig. 3(b)]. For this value of η_s it is necessary to include terms up to seventh order in order to obtain reasonable agreement with the ''exact'' result.

Figure 4 shows the depletion potential at contact, i.e., for $h = 0$ obtained from the ''exact'' result:

$$\Delta W_{pD}(0) = -3\eta_s \frac{1 - 2\eta_s - 2\eta_s^2 - \eta_s^3}{(1-\eta_s)^3}. \tag{3.13}$$

For large values of η_s this is in strong contrast to the Asakura-Oosawa approximation

$$\Delta W_{pA}(0) = -3\eta_s \tag{3.14}$$

and to the third-order results [6] for which the contact value always decreases upon increasing the packing fraction. Equation (3.13) predicts a maximal attraction for $\eta_s = 0.241$ and for $\eta_s > 0.3532$ the contact value is positive so that there is repulsion (see Fig. 4). If we assume a 1% percent error in the Carnahan-Starling equation and a 2% error in the SPT equation ΔW_{pD} will change sign for a packing fraction in the range 0.342 to 0.364.

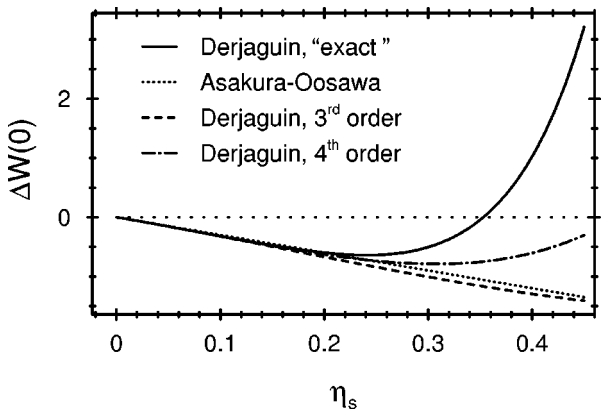

FIG. 4. The normalized depletion potential [Eq. (3.3)] at contact $h = 0$. The full line denotes the ''exact'' Derjaguin approximation [Eq. (3.13)], which has a minimum at $\eta_s = 0.241$ and vanishes at $\eta_s = 0$ and $\eta_s = 0.3532$. The dotted line represents the Asakura-Oosawa (projection) approximation [Eq. (3.14)], which is linear in η_s. The dashed and dashed-dotted lines are the results from the third- and fourth-order expansion [Eq. (3.12)]. Thus, the inclusion of higher-order contributions produces a slow buildup to repulsion at high packing fractions.

C. The wedge approximation for the depletion potential

Using the refined expression for the force between two large fixed spheres [Eq. (2.26)] leads, via Eq. (3.2), to a refined approximation for the depletion potential

$$W_{pw}(h) - W_{pw}(2R_s) = -\pi(R_b + R_s)(2R_s - h)\left[\frac{1}{2}P(\rho_s)(2R_s - h) + \gamma(\rho_s)\left(\frac{R_b + \frac{1}{4}(2R_s + h)}{R_s + R_b}\right)\right], \quad 0 < h < 2R_s. \tag{3.15}$$

Although this formula is very similar to the Derjaguin approximation, the correction becomes very important for large values of s and large values of the packing fraction η_s. This is demonstrated in Table I for two different size ratios $s = 0.2$ and $s = 0.1$ and three different packing fractions. As expected, the contact values from the wedge approximation are more negative than the results of the Derjaguin approximation, indicating a reduction of the repulsive contribution. Note that the normalized depletion potential from the wedge approximation depends on the size ratio and is plotted in Fig. 3(b) for $\eta_s = 0.3665$ and $s = 0.2$. It is significantly less repulsive than the Derjaguin approximation for all $h < 2R_s$.

D. Comparison with simulation data

All the approximations we have discussed, apart from the wedge approximation, are based on the assumption that the contact density difference $\Delta\rho(L)$ [see Eq. (2.8)] does not depend on the size ratio s. They differ only in the subsequent approximation applied to this difference. Thus they can only be accurate for small size ratios. The issue is as follows: Up to which value of s can these approximations be used safely? An obvious way to answer this question is to make a comparison with simulation data [5,7]. In Fig. 9 of Ref. [7] molecular dynamics data for the depletion potential, with $s = 0.1$, are shown for packing fractions $\eta_s = 0.209$, 0.262, 0.314, and 0.367. In the range $0 < h < 2R_s$ the results of the third-order theory of Mao *et al.* [6] are very close to the simulation data. (The third-order theory gives a poor account of the simulation results in the range $2R_s < h$, but this is not germane to the present discussion.) First we concentrate on the case $\eta_s = 0.209$. Since, according to Fig. 3(a), the third-order expansion already provides a good approximation to the ''exact'' Derjaguin result [Eq. (3.9)], we conclude that the latter gives a reasonable account of the simulation data in this case, indicating that the Derjaguin approximation is reliable for a size ratio $s = 0.1$ and for the packing fraction $\eta_s = 0.209$. However, for $\eta_s = 0.367$ Fig. 3(b) shows that the third-order expansion is qualitatively different from the ''exact'' Derjaguin result. Therefore we conclude that the agreement between the predictions of the third-order expansion

TABLE I. The depletion potential at contact $W(0)$ and the height of the depletion barrier $\delta W = \max_h[W(h)-W(0)]$ in units of k_BT for the case of sphere-sphere interactions. η_s is the packing fraction of the small spheres and $s=R_s/R_b$ is the size ratio. W_A denotes the Asakura-Oosawa approximation [Eq. (3.4)] and W_{pA} is the projection approximation of the latter [Eq. (3.6)]. W_{pD} is the Derjaguin approximation [Eq. (3.8)], W_{pw} is the wedge approximation [Eq. (3.15)] and $W_1(0)$ is the result given by Eqs. (5.11) and (5.9) based on the limit $R_b=R_s$. $W_{\rm MC}$ refers to the Monte Carlo results in Ref. [5]. Note that the present theory provides only expressions for the difference $W_{pD}(0)-W_{pD}(2R_s)$ and $W_{pw}(0)-W_{pw}(2R_s)$ and these differences are given in rows 4 and 5 of the table, respectively. However, as argued in the main text, $W_{pD}(2R_s)$ and $W_{pw}(2R_s)$ are both negligible.

	$s=0.2$			$s=0.1$		
η_s	0.116	0.229	0.341	0.116	0.229	0.341
$W_A(0)$	−0.99	−1.95	−2.90	−1.86	−3.66	−5.46
$W_{pA}(0)$	−1.04	−2.06	−3.07	−1.91	−3.78	−5.63
$W_{pD}(0)$	−1.12	−1.91	−0.49	−2.05	−3.50	−0.90
$W_{pw}(0)$	−1.17	−2.23	−1.70	−2.09	−3.82	−2.13
$W_1(0)$	−0.93	−1.98	−3.19	−1.71	−3.62	−5.85
$W_{\rm MC}(0)$	−0.91	−1.84	−2.89	−1.73	−3.69	−5.70
δW_{pD}	1.17	2.54	4.05	2.14	4.66	7.42
δW_{pw}	1.22	2.83	5.01	2.18	4.94	8.37
$\delta W_{\rm MC}$	1.00	2.17	3.69	2.04	4.54	8.24

and the simulation data must be the result of a fortunate cancellation of errors. This comparison demonstrates that the Derjaguin approximation is not valid for this size ratio at this high packing fraction. *A fortiori* this is true for even larger packing fractions.

A similar picture emerges from comparisons with recent Monte Carlo simulations [5]. The authors of this reference provide the values of the depletion potential $W(0)$ for three different values of η_s and for two values of the size ratio, $s=0.1$ and 0.2. At first sight a direct comparison appears difficult, as our present analysis only predicts values for the difference $W(0)-W(2R_s)$. However, from the results of both simulation studies one finds that the values of $W(2R_s)$ are always quite small. $W_{pD}(2R_s)$ has also been calculated within density functional theory [11] and shown to be in the order of 0.01 for a range of η_s. Thus one is able to compare the results of the Monte Carlo simulations for $W_{\rm MC}(0)$ with those from the present approximations by setting $W(2R_s)=0$. Table I shows that for the two lowest packing fractions, $\eta_s=0.116$ and 0.229, the various approximations yield similar results with that of Asakura-Oosawa being closest to the simulation results. On the other hand, for the highest packing fraction $\eta_s=0.341$, the contact values obtained from the Derjaguin approximation $W_{pD}(0)$ and from the simulations differ significantly. $W_{pD}(0)$ is much less negative than $W_{\rm MC}(0)$ for both size ratios. Remarkably the crudest, Asakura-Oosawa, approximation $W_A(0)$ [or $W_{pA}(0)$] yields values that are close to those of the simulations (see also Fig. 5). We regard this as fortuitous [5]. That improving upon the low-density Asakura-Oosawa approximation by introducing an accurate high-density approximation leads to poorer agreement with the simulations reinforces our previous conclusion that the Derjaguin approximation is inappropriate for these size ratios and high packing fractions. This means that replacing the contact density by that in a slit is not justified for size ratios of $s=0.1$ or 0.2. In view of Fig. 1, which is drawn to scale for $s=0.2$, this is not surprising. The introduction of the wedge approximation does imply a decrease in the repulsion at high packing fractions [Fig. 3(b)], and for $\eta_s=0.341$ the values of $W_{pw}(0)$ are substantially more negative than $W_{pD}(0)$ but still underestimate the magnitude of $W_{\rm MC}(0)$ at this packing fraction. While it is very reasonable to expect the Derjaguin approximation to be accurate for $s<0.01$, its application to larger size ratios is not reliable. Finally we define the depletion barrier δW as the difference between the maximum and the contact value of the depletion potential. This quantity does not require knowledge of $W(2R_s)$. The results for δW from the Derjaguin approximation, the wedge approximation, and the simulation data are also given in Table I. Both approximations predict the cor-

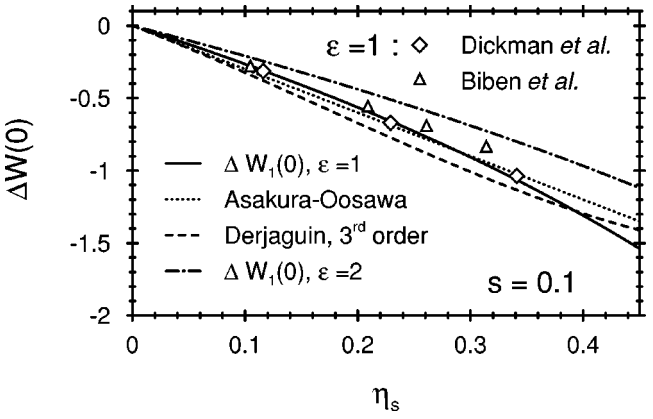

FIG. 5. The normalized depletion potential [Eq. (3.3)] at contact $h=0$. The full and the dashed-dotted line denote $\Delta W_1(0)$ [Eq. (5.12)] for the case of a sphere-sphere ($\epsilon=1$) and a sphere-wall ($\epsilon=2$) interaction, respectively. The dotted line represents the Asakura-Oosawa (projection) approximation [Eq. (3.14)] and the dashed line is the result from the third-order expansion [Eq. (3.12)]. The diamonds and the triangles denote simulation results, for $s=0.1$ and $\epsilon=1$, of Dickman *et al.* [5] and Biben *et al.* [7], respectively. The results obtained in Ref. [5] are also listed in Table I. For the present plot these data have been normalized by a factor of $2s/(1+s)=0.1818$.

rect variation of δW with η_s. However, the above discussion of $W(0)$ shows that the approximations do not account for the *shape* of the depletion potential found in the simulations at the higher values of η_s.

IV. DEPLETION POTENTIAL FOR MORE GENERAL FLUIDS

So far we have considered only the case of hard obstacles immersed in a hard sphere fluid. The considerations presented in the Appendix are more general and allow for the presence of soft interaction potentials. First, we focus on two hard obstacles (i.e., two hard spheres of radius R_b or a hard sphere in front of a hard wall) immersed in a fluid of small spherical particles, which interact with each other via an arbitrary potential function. The obstacles are called hard if their interactions with the small particles are infinitely repulsive below a suitably chosen distance R_b+R_s and zero otherwise. For such models Eqs. (2.4) and (2.5) remain valid, with an appropriate definition of (R_b+R_s). In this case the various approximations, which were introduced in Secs. II and III, can be implemented straightforwardly. For example, the Derjaguin approximation, which should be exact in the limit of $s\to 0$, Eq. (2.21) remains valid with $P(\rho_s,T)$ and $\gamma(\rho_s,T)$ referring to the pressure and interfacial tension of the particular fluid under consideration. As indicated, P and γ and thus the depletion potential have gained a temperature dependence. If the interaction potential between the small particles contains both attractive and repulsive parts, the depletion potential given by Eq. (3.8) exhibits a rather different dependence on ρ_s from that of the hard sphere fluid, because both $P(\rho_s,T)$ and $\gamma(\rho_s,T)$ reflect the presence of attractive forces. In general $P(\rho_s)$ will be smaller than for a fluid of (small) hard spheres of the same density ρ_s so that its contribution to the depletion potential will be less attractive. On the other hand, $\gamma(\rho_s,T)$ can be less negative (it may be even positive) than for hard spheres at a hard wall so that a net attraction can still occur. Nevertheless some results of Sec. III still hold. The virial expansion of the surface tension reveals [25] that for any spherically symmetric particle-particle interaction the linear term vanishes. Thus it also follows in a more general fluid that the low density behavior is dominated by the pressure term. Finally, if the potential exerted by obstacle 2 is soft one should employ Eq. (A4) for the depletion force, which now depends *explicitly* on the potential V_2.

The case of nonspherical particles introduces new features. These have been considered by Asakura and Oosawa [26] and more recently by Mao *et al.* [27] who have investigated depletion forces and other properties for hard rods between hard parallel plates.

V. THE LIMIT $R_b=R_s$

In this section we consider the special case in which the radius R_b of the fixed sphere 2 equals that of the (small) spheres. We shall use results obtained in this limit in order to suggest an alternative approximation for the depletion potential that will become exact in the limit $s=R_s/R_b\to 1$.

To this end we consider a fluid subject to an external potential $V_1(\mathbf{R})$ [$V_2\equiv 0$ in Eq. (2.1)]. For the system to be in thermal equilibrium the net force on a fluid particle at position $\mathbf{R}$ must vanish, i.e.,

$$-\beta^{-1}\nabla\ln\rho(\mathbf{R})-\nabla V_1(\mathbf{R})+\mathbf{F}(\mathbf{R})=0, \tag{5.1}$$

where $\rho(\mathbf{R})$ is the equilibrium density profile in the presence of $V_1(\mathbf{r})$ and $\mathbf{F}(\mathbf{R})$ is the force arising from the interactions with the other fluid particles. In the case of pairwise interactions, described by a pair potential $\Phi(|\mathbf{R}|)$, the latter force is given by

$$\mathbf{F}(\mathbf{R})=-\int d^3R'\nabla\Phi(|\mathbf{R}-\mathbf{R}'|)\rho(\mathbf{R}')g(\mathbf{R},\mathbf{R}'), \tag{5.2}$$

where $g(\mathbf{R},\mathbf{R}')$ is the pair correlation function of the inhomogeneous fluid; Eq. (5.1) is then the first Born-Green-Yvon equation [28]. According to the Percus test particle theorem $\rho(\mathbf{R}')g(\mathbf{R},\mathbf{R}')$ is the density profile of the system subject to an additional external potential $V_2(\mathbf{R})=\Phi(|\mathbf{R}|)$ due to a fluid particle fixed at the position $\mathbf{R}$ [28]. Therefore the force in Eq. (5.2) reduces to that given by Eq. (A4). Thus $\mathbf{F}(\mathbf{R})$ is equivalent to the force defined in Eq. (2.3) in the special case where $V_2(\mathbf{R})=\Phi(|\mathbf{R}|)$ and the corresponding potential $W(\mathbf{R})$ [see Eq. (3.1)] can be obtained from Eq. (5.1),

$$-W(\mathbf{R})=V_1(\mathbf{R})+\beta^{-1}\ln\frac{\rho(\mathbf{R})}{\rho_s}, \tag{5.3}$$

with the boundary conditions $V_1(\infty)=0$ and $\rho(\infty)=\rho_s$. Note that here $\rho(\mathbf{R})$ denotes the density profile of the system with $V_2\equiv 0$. Thus one has

$$\rho(\mathbf{R})=\rho_s\exp\{-\beta[V_1(\mathbf{R})+W(\mathbf{R})]\} \tag{5.4}$$

and $W(\mathbf{R})$ is the work that must be performed against the interparticle forces in order to bring a fluid particle from infinity to the fixed position $\mathbf{R}$.

If the potential $V_1(\mathbf{R})$ is due to that of an identical fixed particle, i.e., $V_1(\mathbf{R})=\Phi(|\mathbf{R}|)$, the density profile is given by the Percus test particle theorem, i.e., $\rho(\mathbf{R})=\rho_s g(R=|\mathbf{R}|)$, where $g(R)$ is the radial distribution function of the homogeneous fluid of density ρ_s and Eq. (5.4) reduces to

$$g(R)=\exp\{-\beta[\Phi(R)+W(R)]\}. \tag{5.5}$$

For this particular situation $\Phi(R)+W(R)$ is the potential of mean force. Thus for case (a), i.e., a hard sphere fixed at the origin, the depletion potential between two hard spheres identical to those constituting the fluid is given by

$$\beta W^{(a)}(h)=-\ln g_{\rm hs}(2R_s+h), \quad h>0. \tag{5.6}$$

If the potential $V_1(\mathbf{R})=V_1(h)$ is that of a planar wall,

$$\beta[W(h)+V_1(h)]=-\ln[\rho_{\rm wall}(h)/\rho_s], \tag{5.7}$$

where $\rho_{\rm wall}(h)$ is the density profile of the fluid near the wall. In case (b), i.e., a planar hard wall, this reduces to

$$\beta W^{(b)}(h)=-\ln[\rho_{\rm hw}(h)/\rho_s], \quad h>0, \tag{5.8}$$

where $\rho_{\rm hw}(h)$ is the density profile of the fluid near a hard wall. Note that Eqs. (5.7) and (5.8) are valid for any fluid, not only for a hard sphere fluid.

The contact value ($h=0$) of the depletion potential for cases (a) and (b) can be related to the pressure $P(\rho_s)$ of the fluid via the virial expression and the wall sum rule, respectively, yielding

$$\beta W^{(a)}(0) = -\ln\left[\frac{1}{4\eta_s}\left(\frac{\beta P(\rho_s)}{\rho_s}-1\right)\right] \tag{5.9}$$

and

$$\beta W^{(b)}(0) = -\ln\left(\frac{\beta P(\rho_s)}{\rho_s}\right). \tag{5.10}$$

In the limit $\eta_s \to 0$ the ratio $\epsilon_1 = W^{(b)}(0)/W^{(a)}(0)$ is given by the ratio $B_2^2/B_3 = 8/5 = 1.6$, where B_2 and B_3 are the second and third virial coefficients, respectively, of the pressure. Upon increasing the density the ratio decreases very slowly. For example at $\eta_s = 0.45$, for which the Carnahan-Starling equation of state [Eq. (3.10)] yields $\beta P/\rho_s = 9.38$, one has $\epsilon_1 = 1.46$.

In the same spirit as the Derjaguin approximation is based on exact results valid in the limit $s=0$, we propose the use of Eqs. (5.6) and (5.8), which are exact for $s=1$, in order to estimate the depletion potential for s close to 1. Since the dependence of $W(h)$ on the size ratio is not known in detail, we assume the same dependence as in the previous (projection) approximations and propose the following approximation $W_1(h)$, which reduces to the exact result $W^{(a,b)}(h)$ in the limit $s \to 1$:

$$W_1(h) = \frac{(R_b+R_s)}{2R_s} W^{(a,b)}(h). \tag{5.11}$$

Thus the normalized potential [Eq. (3.3)] carries no explicit dependence on s and is given by

$$\Delta W_1(h) = \begin{cases} -\ln\left(\dfrac{g_{\rm hs}(2R_s+h)}{g_{\rm hs}(4R_s)}\right), & \epsilon = 1 \\ -\dfrac{1}{2}\ln\left(\dfrac{\rho_{\rm hw}(h)}{\rho_{\rm hw}(2R_s)}\right), & \epsilon = 2. \end{cases} \tag{5.12}$$

In contrast to previous approximations this, normalized, depletion potential is different for case (a) and case (b). Moreover, this approximation provides $W(h)$ for all $h>0$. It is shown for $\epsilon=1$ in Fig. 3(b), taking the radial distribution function $g_{\rm hs}(h)$ from the Percus-Yevick approximation. Comparing the ''exact'' Derjaguin approximation (full line) with the wedge approximation (dashed-double-dotted line, plotted for $s=0.2$) and with $\Delta W_1(h)$ (dashed-triple-dotted line) one observes a systematic decrease of the repulsive part of the potential. Since the two limits $s=0$ and $s=1$ are described exactly by the Derjaguin result and by Eq. (5.12), respectively, one is inclined to use them in order to estimate the potential close to these limits. However, as one can see in Fig. 3(b) at this density the limiting values of the normalized depletion potential differ significantly so that there is no obvious starting point for the description of systems with intermediate size ratios. In Ref. [7] the authors report a good agreement between their simulation data for $s=0.1$ and the results of the third-order expansion [6], given by the dashed line in Fig. 3(b). $\Delta W_1(h)$ is rather close to the simulation results; surprisingly it seems to be a reasonable approximation even for this low size ratio $s=0.1$. In Table I $W_1(0)$ is compared with the other approximations and with MC simulation data for $s=0.2$ and $s=0.1$. In both cases it is in good agreement with the simulations, even at high densities.

In Fig. 5 for a range of packing fractions η_s, $\Delta W_1(0)$ is compared with the results of the Asakura-Oosawa (projection) approximation [Eq. (3.6)], the simulation results obtained in Refs. [5] and [7], and with the third-order expansion of the Derjaguin result. All of these approximations predict that $\Delta W(0)$ is decreasing monotonically with increasing density, which is in sharp contrast to the ''exact'' Derjaguin result (see Fig. 4). The comparison with the results of both simulations shows that the sphere-sphere ($\epsilon=1$) result in Eq. (5.12) provides a fair account of the density dependence of the contact value. The wall-sphere ($\epsilon=2$) result in Eq. (5.12) predicts a somewhat less attractive *normalized* potential at contact. (Note the factor $\frac{1}{2}$, which arises in the definition of ΔW.) The presence of the logarithm in the expression for $\Delta W_1(h)$ implies that although the pressure $P(\rho_s)$ is increasing very rapidly with increasing density ρ_s, $\Delta W_1(0)$ has a much weaker—roughly linear—dependence on ρ_s.

VI. THERMODYNAMICS, PHASE SEPARATION, AND STRUCTURE OF BINARY HARD SPHERE MIXTURES

So far we have considered the depletion potential between an isolated pair of big spheres or a big sphere and a wall. In this section we turn our attention to bulk mixtures of big and small hard spheres and ask whether the results derived for the depletion potential have relevance for the equilibrium properties of such mixtures. These model systems have attracted much attention. The phase behavior has been investigated by both simulation and theoretical techniques and for certain size ratios, typically $0.4 \lesssim s \lesssim 0.6$, the solid-fluid and solid-solid phase diagrams are well established. Depending on the value of s, different crystalline phases may exist, which coexist with each other and/or with a fluid phase [29]. A more contentious and intriguing issue is whether fluid-fluid phase separation can occur in this model. Lebowitz and Rowlinson [30] showed that within the Percus-Yevick closure approximation, hard spheres mix at all concentrations for any value of s. Much later, Biben and Hansen [31,32] found, based on numerical solutions of integral equations using an improved closure approximation, strong evidence for a spinodal instability when $s \lesssim 0.2$ and attributed this to attractive depletion forces. That study spurred many subsequent investigations (see the summaries in Refs. [7] and [33]). However, it is probably fair to argue that it is still an open question as to whether fluid-fluid phase separation does occur for the binary hard-sphere mixture [34]. It certainly does occur for a lattice model of a binary mixture of parallel hard cubes [35], which demonstrates that entropic effects alone suffice to drive the phase separation. The matter is not settled because for the continuum case ergodic problems for small size ratios are severe; computer time is spent on moving the small spheres around whereas displacing a big sphere is a move that is rarely accepted when the density of the small spheres is large. Given the difficulties of treating both

species on equal footing, it is tempting to follow the standard procedure of statistical physics and construct an effective Hamiltonian $H_{bb}^{\rm eff}$ for the big ''particles'' by integrating out the degrees of freedom of the small spheres. Simulations, or theoretical analyses, can then be performed for this effective one-component system. Formally one has

$$H_{bb}^{\rm eff}(\{\mathbf{R}_i\})=H_{bb}^{\rm hs}(\{\mathbf{R}_i\})+A_s(\{\mathbf{R}_i\}), \tag{6.1}$$

where $H_{bb}^{\rm hs}(\{\mathbf{R}_i\})$ denotes the Hamiltonian of the bare big hard spheres and $A_s(\{\mathbf{R}_i\})$ is the Helmholtz free energy of the inhomogeneous distribution of small spheres in the presence of a configuration of N_b big spheres located at fixed positions $\{\mathbf{R}_1,\ldots,\mathbf{R}_{N_b}\}$. Finding suitable approximations for A_s is not straightforward for this particular problem. In the general case, i.e., arbitrary values of s and arbitrary densities ρ_s and ρ_b, there is no small parameter that permits a natural perturbative approach to the calculation of A_s. When the density ρ_b is low one might expect the approximation of pairwise additive potentials to be reasonable. Moreover, when the size ratio $s<0.154$ [7,36] there are no configurations in which a small sphere can be in simultaneous contact with three big spheres. This rules out one important source of many-body effects. (Within the Asakura-Oosawa approximation this is the only source and it follows that there are no three-body or higher-order potentials for $s<0.154$ [36].) Biben *et al.* [7] conclude from the analysis of their simulation data that pairwise additivity should be an excellent approximation for $s\lesssim 0.1$, even at high densities. For larger ratios one should expect this approximation to break down. In the present discussion we restrict ourselves to small values of s and assume that the potential energy of the big particles is $\Sigma_{i<j}\Phi_{bb}(|\mathbf{R}_i-\mathbf{R}_j|)$ with the effective pair potential

$$\Phi_{bb}(r)=\begin{cases}\infty, & r<2R_b\\ W(r-2R_b), & r>2R_b,\end{cases} \tag{6.2}$$

where $W(r-2R_b)\equiv W(h)$ is the depletion potential between two big spheres. $W(h)$ depends on ρ_s but not on ρ_b. For the subsequent discussion we choose the Derjaguin result [Eq. (3.8)] because this becomes exact as $s\to 0$, i.e., we set $W(h)=W_{pD}(h)-W_{pD}(2R_s)$. Since $W_{pD}(h)$ is not available for $h>2R_s$, we assume, for simplicity, $W(h)=0$ for $h>2R_s$. Although the results of density functional calculations [11] and simulations [5,7] show that $W(h)$ has weak oscillations in this range, omitting these should not have any dramatic effect on the properties of the mixture. Thus we have $\Phi_{bb}(r)=0$ for $r>2(R_b+R_s)$ and the resulting pair potential is of a type similar to that considered previously in Refs. [37] and [36] whose authors investigated phase separation in models of colloid-polymer mixtures. Those authors used the Asakura-Oosawa approximation for the depletion potential. We examine the consequences for the hard-sphere mixture of employing a more accurate theory, valid also for large values of the packing fraction η_s, for which the Asakura-Oosawa approximation fails.

In order to obtain some physical insight into thermodynamic properties, we treat the depletion potential as a perturbation on the hard-sphere potential. The first-order approximation in this perturbation approach for the Helmholtz free energy per big sphere is

$$\frac{A(\rho_b,\rho_s)}{N_b}=\frac{A^{\rm hs}(\rho_b)}{N_b}+2\pi\rho_b \times\int_{2R_b}^{2(R_b+R_s)}dr\; r^2 W_{pD}(r-2R_b)g^{\rm hs}(r;\rho_b), \tag{6.3}$$

where $g^{\rm hs}(r;\rho_b)$ is the radial distribution function of the big hard sphere fluid and $A^{\rm hs}(\rho_b)$ is the Helmholtz free energy for the same homogeneous fluid of density $\rho_b=N_b/V$. Since $R_s\ll R_b$, $g^{\rm hs}(r;\rho_b)$ is almost constant over the range of the integration and we can approximate it by its contact value $g^{\rm hs}(2R_b;\rho_b)$. Then the integral can be easily performed and we find

$$\frac{\beta A(\rho_b,\rho_s)}{N_b}=\ln(\Lambda^3\rho_b)-1+\frac{\eta_b(4-3\eta_b)}{(1-\eta_b)^2} -3\pi\eta_b g^{\rm hs}(2R_b;\rho_b) \times\left(\frac{1}{3}\tilde{P}(\rho_s)\alpha_P(s)-2\tilde{\gamma}(\rho_s)\alpha_\gamma(s)\right), \tag{6.4}$$

where $\eta_b=4\pi\rho_b R_b^3/3$ is the packing fraction of the big spheres and where we have used the Carnahan-Starling formula [9] for the hard-sphere free energy; Λ is the thermal de Broglie wavelength of the big spheres. For small s the quantities

$$\alpha_P(s):=1+\frac{1}{2}s+\frac{1}{10}s^2 \tag{6.5}$$

and

$$\alpha_\gamma(s):=1+\frac{2}{3}s+\frac{1}{6}s^2 \tag{6.6}$$

depend weakly on the size ratio and for $s<0.1$ it causes little error to replace them by unity. Thus, the last term in Eq. (6.4) is determined essentially by the combination $\frac{1}{3}\tilde{P}(\rho_s)-2\tilde{\gamma}(\rho_s)$, which is similar to the one that determines the normalized depletion potential at contact, i.e., $\frac{1}{2}\tilde{P}(\rho_s)-2\tilde{\gamma}(\rho_s)$ [see Eq. (3.9)].

To first order in η_s, in Eq. (6.4), only the pressure term contributes, $\tilde{P}(\rho_s)\sim 6\eta_s/\pi$, and the free energy reduces to that which one would obtain from using the Asakura-Oosawa depletion potential in the projection approximation. In this case the last term in Eq. (6.4) is always negative, reflecting the fact that the potential $W_{pA}(h)$ is always attractive. However, as demonstrated in Sec. III, at higher values of η_s the surface tension contribution $\tilde{\gamma}(\rho_s)$ becomes equally important and the variation with η_s of the final term in the free energy should be similar to that of $\Delta W(0)$ in Fig. 4. But the upturn sets in at smaller values of η_s, because the

coefficient of $\tilde{P}(\rho_s)$ is 1/3 instead of than 1/2. This means that the ''exact'' Derjaguin result predicts a significantly smaller attractive contribution to the free energy for $\eta_s \gtrsim 0.1$ and a repulsive contribution for $\eta_s > 0.222$. This observation has clear repercussions for phase separation. If we calculate the compressibility by differentiating Eq. (6.4) with respect to ρ_b at fixed η_s and take the Percus-Yevick value for $g^{\rm hs}(2R_b;\rho_b)$, there is no divergence within the fluid range of either packing fraction, i.e., there is no indication of a fluid-fluid spinodal. However, Eq. (6.4) is a crude approximation to the free energy of this particular model fluid and better approximations or simulations should be employed to test this prediction. Note also that the packing fraction η_s, which enters into the effective Hamiltonian, should reflect the fact that there is less free volume available for the small spheres when there is a macroscopic number N_b of large spheres present in the bulk fluid [7]. What emerges from these considerations is that the variation of the free energy with η_s seems to depend sensitively on the approximation used for the depletion potential in the range of η_s where fluid-fluid separation might occur for hard-sphere mixtures [7] and different approximations could easily produce very different results.

We turn now to the structure of the fluid of big particles interacting via the effective pair potential $\Phi_{bb}(r)$. The shape of the corresponding radial distribution function $g_{bb}(r)$ and of the structure factor $S_{bb}(k)$ reflect the form of the depletion potential W. If the latter is strongly attractive, we have a very ''sticky'' pair potential and the contact value $g_{bb}(2R_b)$ is much larger than the contact value $g^{\rm hs}(2R_b;\rho_b)$ for the one-component hard-sphere fluid at the same density ρ_b. This is one of the reasons one must be cautious in using the perturbative approach presented in Eq. (6.3). The simulation studies for binary mixtures in Ref. [7] confirm this conjecture; they yield $g_{bb}(2R_b) > 20$ for $s = 0.1$, $\eta_s = 0.1$, and $\eta_b = 0.25$. The new prediction that emerges from the present study is that as η_s increases to larger values the depletion potential actually becomes more repulsive—at least within the context of the Derjaguin approximation applicable to small values of s. This means that a new characteristic length scale $\sim 2R_b + R_s$ may become important. No such length arises in the Asakura-Oosawa approximation for which W is attractive at all distances. Thus we argue that as η_s increases a characteristic feature such as an additional maximum in $S_{bb}(k)$ should develop near $k = 2\pi/(2R_b + R_s)$, whereas for small η_s there should only be the peak located near π/R_b. A strongly attractive depletion potential will also act to increase $S_{bb}(0)$, which is proportional to the osmotic compressibility, above the corresponding one-component hard-sphere value at the same value of η_b. Such behavior of $S_{bb}(0)$ is already visible in the Percus-Yevick results for binary mixtures [38], for which it is interpreted as evidence for depletion attraction. If the depletion potential varies with η_s as predicted by the Derjaguin approximation this will lead to behavior of $S_{bb}(0)$ very different from that which emerges from the Asakura-Oosawa approximation. Within the latter $S_{bb}(0)$ should always increase with η_s whereas within the former $S_{bb}(0)$ should decrease when the depletion potential becomes repulsive. These expectations can be tested, e.g., by calculating $S_{bb}(0)$ within the framework of the random phase approximation (RPA), which has been successful in describing the small momentum behavior of the structure factors of simple liquids and liquid metals [39,40]. The RPA asserts that for a pair potential of the type given in Eq. (6.2) the direct correlation function can be approximated by

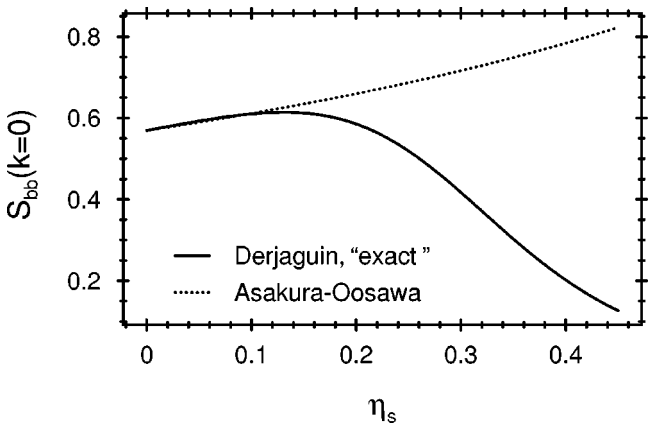

FIG. 6. The structure factor S_{bb} at $k = 0$ for a range of packing fractions η_s, calculated within RPA [Eqs. (6.7) and (6.8)]. The small-hard-sphere fluid has a fixed packing fraction $\eta_s = 0.1$. The full and the dotted line correspond to the ''exact'' Derjaguin and Asakura-Oosawa approximation, respectively, for the underlying depletion potential. The Derjaguin approximation predicts a maximum and a turning point the Asakura-Oosawa approximation yields a monotonic increase.

$$c_{bb}(r;\rho_b) = c^{\rm hs}(r;\rho_b) - \beta W(r - 2R_b), \tag{6.7}$$

with $W \equiv 0$ for $r < 2R_b$. $c^{\rm hs}(r;\rho_b)$ is the hard-sphere direct correlation function, which can be obtained from the Percus-Yevick approximation. The structure factor is then given by the Ornstein-Zernike relation

$$S_{bb}(k) = \frac{1}{1 - \rho_b \hat{c}_{bb}(k;\rho_b)} \tag{6.8}$$

with $\hat{c}_{bb}(k;\rho_b) = \int d^3r \exp(i\mathbf{k}\cdot\mathbf{r}) c_{bb}(r;\rho_b)$. In Fig. 6 we show $S_{bb}(0)$, calculated from Eqs. (6.7) and (6.8), as a function of η_s for a fixed big sphere packing fraction $\eta_b = 0.1$. These results support the expectations stated above. $S_{bb}(0)$ increases monotonically for the Asakura-Oosawa approximation. By contrast it reaches a maximum near $\eta_s = 0.13$ and decreases rapidly at higher values when the ''exact'' Derjaguin result for the depletion potential is used. There is no indication of a spinodal, i.e., the compressibility—proportional to $S_{bb}(0)$—does not diverge, for either potential. It is well known that although the RPA does not provide an accurate description of the short wavelength behavior $k \gtrsim \pi/R_b$ in simple liquids, it usually provides a realistic account of the long-wavelength behavior. The reliability of the RPA for the present model potential, which is very different from the Lennard-Jones or liquid metal pair potentials, is, of course, uncertain, even for $k \to 0$.

To summarize we suggest that both the pairwise structure and the thermodynamic properties of the hard-sphere mixture should reflect the variation of the depletion potential with η_s. The specific predictions listed here await tests by computer simulations of the effective one-component fluid as

well as experimental tests such as by small angle neutron scattering from suitable chosen colloidal solutions resembling closely hard sphere mixtures.

VII. SUMMARY AND DISCUSSION

In this paper we have examined the statistical mechanics of the so-called depletion potential, i.e., the effective potential that arises between a large hard sphere of radius R_b and a second obstacle at distance h immersed in a fluid composed of particles with radius R_s and number density ρ_s. Defining the force between the two obstacles as minus the derivative with respect to the separation h of the grand potential we have shown that this force depends only on the density profile of the fluid at contact with the hard sphere. Our derivation demonstrates that this result is valid for an arbitrary second obstacle, for density profiles obtained within the context of density-functional approximations, and for any simple fluid, not only hard spheres. By considering various approximations for the density profile we have constructed a variety of approximations for the force between obstacles. The main results can be summarized as follows:

(1) The simplest approximation leads to the well-known Asakura-Oosawa result for the depletion force.

(2) More sophisticated approximations lead to new results for the force. The Derjaguin approximation [Eq. (2.21)] is of particular significance because it allows one to express the force in terms of the bulk fluid pressure and the hard-wall—fluid surface tension, which are both readily accessible even for high fluid densities. This approximation is valid for small size ratio $s=R_s/R_b \ll 1$. The wedge approximation [Eq. (2.26)] relieves some of the restrictions placed on a fluid by confining it to a slit, an assumption inherent in the Derjaguin approximation.

(3) Section III concentrates on the depletion potential that arises for two hard obstacles (two big hard spheres or a hard sphere and a hard wall) in a small-hard-sphere fluid. Within the Derjaguin approximation we discuss the consequences of an explicit formula for the potential $W(h)$ in the regime $0<h<2R_s$, where R_s is the radius of the small spheres. In the limit of low packing fractions $\eta_s=4\pi\rho_s R_s^3/3\to 0$, it reduces to the Asakura-Oosawa approximation but for large η_s it leads to very different depletion potentials. Indeed, for $\eta_s>0.3532$ the contact value $W(h=0)$ is positive whereas the Asakura-Oosawa approximation predicts strong attraction, i.e., the contact value is negative and decreases linearly with η_s (see Fig. 4). Our result contradicts the assumption that the depletion potential for hard-sphere fluids is always attractive.

(4) Recent work by Mao *et al.* [6] has also emphasized that the depletion potential is less attractive than that obtained by Asakura and Oosawa. We have shown that their theory is equivalent to a third-order expansion of our ''exact'' Derjaguin formula in powers of η_s and that this third-order expansion is not even qualitatively correct for $\eta_s \gtrsim 0.3$.

(5) The comparison of our Derjaguin results with simulation data [5,7] for W, obtained for hard spheres with size ratios $s=0.1$ and 0.2, shows that there are significant differences for large values of η_s. We conclude that the Derjaguin approximation is only valid for very small values of s, for which replacing the contact density by that for a slit is fully justified. At high packing fractions, $\eta_s>0.3$, the wedge approximation performs much better for $s=0.1$ and 0.2 (Table I). We argue that the apparent agreement between simulation data and results of the third-order theory of Mao *et al.* [6] is caused by a fortuitous cancellation of errors.

(6) In Sec. V we have considered the particular limit in which the fixed spherical obstacle is a fluid particle itself. In this case the depletion potential is given in terms of the logarithm of the density profile of the fluid in the absence of the obstacle [see Eq. (5.3)]; for the hard sphere fluid the sphere-sphere depletion potential reduces to the potential of mean force. This result for the limit $s=1$ has been used as a motivation for introducing a new approximation for $s<1$ [see Eq. (5.12)]. The comparison with simulation data shows that this approximation is reasonably good even for size ratios as small as $s=0.1$. Thus, there are approximations for the depletion potential available that are exact in the limits $s\to 0$ or $s\to 1$. They differ substantially from each other and it is not clear which of them is more appropriate or how one should interpolate between them for intermediate values of s. Further simulation studies of the type reported in Refs. [5] and [7] for smaller values of s are necessary to ascertain the regime of validity of the Derjaguin approximation.

(7) In Sec. VI we showed that our approximations for the depletion potential have implications for the structure and the thermodynamic properties of binary hard-sphere mixtures and, in particular, may shed new light on the long standing issue of fluid-fluid phase separation in these systems.

In the following we return to the question of whether the concept of depletion forces and our present results can be carried over to more general fluids (see Sec. IV). To this end we consider a model fluid that has an arbitrary, but short-ranged particle-particle interaction but a hard-sphere interaction with the wall, i.e., the potential is infinite if the center of the particle is closer than R_s to the wall and is zero otherwise. Thus, if two walls come closer to each another than $2R_s$ all particles are expelled, i.e., depletion occurs. In discussing the depletion force for this model fluid, we restrict ourselves to the Derjaguin approximation, but the other results of Sec. II are also applicable. In this approximation the depletion force between the two obstacles is determined by the balance between the surface tension γ and the pressure P of the model fluid. Polymers are natural candidates for a description in terms of such a model fluid. Indeed the depletion effect was introduced orginally [1,26,37] in the context of mixtures of colloids and nonadsorbing polymers. The colloid-polymer potential is assumed to be of a hard sphere type with a radius R_s, which is determined by the radius of gyration. In reality the colloid-polymer potential is soft but provided its range is small compared with the colloidal radius R_b and with R_s, the approximation of a hard-sphere interaction with the wall should be reasonable. The more subtle question is how to model the polymer-polymer interactions in terms of an effective potential. Near the theta temperature, where even the intramolecular excluded volume effects become negligible, it is reasonable to ignore all polymer-polymer interactions. In this case the surface tension of the model fluid vanishes and the pressure is just that of an ideal gas. Then the ''exact'' Derjaguin formula $W_{pD}(h)$ [Eq. (3.9)] reduces to the Asakura formula $W_{pA}(h)$

[Eq. (3.7)], which, for this model, should apply even for high densities ρ_s. This was the scenario investigated in these early papers [1,26,37]. For other temperatures excluded volume effects should be important and one might expect the theories that are developed here to be more appropriate. One might obtain the surface tension and the pressure from direct measurements on the actual investigated polymers and use these in the ''exact'' Derjaguin formula [Eq. (3.9)]. In this way the polymer-polymer interaction is fully and properly taken into account (within the context of the Derjaguin approximation) and the only remaining assumption is that the interaction with the wall is hard-sphere-like.

To what extent are these theories relevant to experiment? Measurements of the depletion force [41] or the potential barrier height [42] for a colloidal particle near a wall now seem feasible and the results of such experiments can, in principle, be compared with those from theory. From measurements of diffusion coefficients in a binary colloid mixture, barrier heights δW have been extracted [42] for packing fractions $0.1 \lesssim \eta_s \lesssim 0.3$ and for a size ratio $s \approx 0.035$. The meassured barrier heights were much smaller ($\beta \delta W \sim 2$) than all theoretical predictions ($\beta \delta W > 10$). The source of this discrepancy is not known [5]. On the other hand there are laser radiation pressure experiments [41] that measure the minimum laser intensity required to blow off a polystyrene latex particle trapped near the wall as a function of the polymer concentration. These results [41] have been interpreted as being in agreement with the Asakura-Oosawa approximation for the depletion force. However, one should note that in both experiments there are possible influences from screened Coulomb forces and it is probably premature to argue that the theoretical and experimental results are in conflict.

It follows from the discussion in Sec. VI that the thermodynamic properties and the structure of a bulk colloidal suspension should depend on the depletion potential and should reflect how this varies with the concentration of the small spheres (polymer). If the attraction is large enough phase separation can occur in the colloid-polymer mixture. The corresponding studies have led to a large literature on this subject (see, e.g., Ref. [33] for a summary). Work that is close in spirit to this aspect of the present study is that of Gast *et al.* [36] who analyzed the phase behavior following from an effective pair potential model. Their model is equivalent to Eq. (6.2) with W given by the Asakura-Oosawa approximation. It was treated using second-order perturbation theory based on the big-hard-sphere reference fluid. The authors found a fluid-solid phase separation for most size ratios and polymer concentrations relevant to experiments. For $s > 0.3$ an additional fluid-fluid transition appeared. In the light of the present work it is clearly of interest to carry out similar investigations, but employing simulation techniques for potentials based on the approximations developed here. From such studies one might learn how sensitive the phase behavior is to the details of the depletion potential. There are, of course, the issues of how reliable the effective *two*-body Hamiltonian is and how to take proper account of the density dependence when calculating the free energy (see Sec. VI). The corresponding calculation of the pair correlation function and of the structure factor should be equally revealing. Recently Ye *et al.* [43] have measured $S_{bb}(k)$, the colloid-colloid structure factor, by matching the neutron scattering length density of the solvent with that of the polymer, for varying polymer concentrations and a series of colloid concentrations. They analyze their data by using the random phase approximation (RPA) to calculate $S_{bb}(k)$ for a pairwise potential Φ_{bb} [Eq. (6.2)] with the *form* of W given by the Asakura-Oosawa approximation. In this way they obtained good fits to their scattering data for a wide range of mixtures using the amplitude of the depletion potential as the only free parameter. For small concentrations the latter increases linearly with polymer concentration, as predicted by the Asakura-Oosawa approximation, but the slope is a factor of 6 smaller than the theoretical value, i.e., the depletion potential is much weaker than predicted. It would be of much interest to have the same type of data for systems where the size ratio s is very small so that one could test the applicability of the Derjaguin approximation.

ACKNOWLEDGMENTS

We thank M. Dijkstra, A. Hanke, H.N.W. Lekkerkerker, and H. Löwen for helpful discussions. R.E. is grateful for the hospitality of the Physics Department of the University of Wuppertal.

APPENDIX

Density functional theory is based on the property that for any fluid that is exposed to an arbitrary external potential $V(\mathbf{R})$ all measurable equilibrium quantities are unique functionals of the number density profile $\rho(\mathbf{R})$ which minimizes the grand canonical free energy functional

$$\Omega([\rho(\mathbf{R})];\mu,T) = F([\rho(\mathbf{R})];T) - \int d^3R[\mu - V(\mathbf{R})]\rho(\mathbf{R}) \tag{A1}$$

at a given chemical potential μ and temperature $T = 1/(k_B\beta)$. The external potential determines the volume over which the integral is performed. $F[\rho] = F_{\mathrm{id}}[\rho] + F_{\mathrm{ex}}[\rho]$ is the intrinsic Hemholtz free energy functional consisting of an ideal gas part, F_{id}, and an excess part F_{ex}.

Upon differentiating the equilibrium grand canonical potential $\Omega([\rho(\mathbf{R})];\mu,T)$ arising from Eq. (A1) one obtains via the chain rule

$$\frac{\delta\Omega}{\delta V(\mathbf{R})} = \rho(\mathbf{R}) + \int d^3R' \left\{ \frac{\delta F[\rho]}{\delta\rho(\mathbf{R}')} - [\mu - V(\mathbf{R}')] \right\} \times \frac{\delta\rho(\mathbf{R}')}{\delta V(\mathbf{R})}. \tag{A2}$$

If $\rho(\mathbf{R})$ is the equilibrium density distribution, the expression within the curly brackets vanishes. This is valid even for *approximations* of the functional $F_{\mathrm{ex}}[\rho]$. For the case studied in Sec. II the external potential $V(\mathbf{R};h)$ in Eq. (2.1) depends parametrically on the separation h so that with Eq. (A2) one has

$$\left(\frac{\partial\Omega}{\partial h}\right)_{T,\mu,A} = \int d^3R \frac{\delta\Omega}{\delta V(\mathbf{R};h)} \frac{\partial V(\mathbf{R};h)}{\partial h} = \int d^3R\ \rho(\mathbf{R})\left(-\frac{1}{\beta}\exp\beta V(\mathbf{R};h)\right)\frac{\partial \exp[-\beta V(\mathbf{R};h)]}{\partial h}$$

$$= -\frac{1}{\beta}\int d^3R\ n(\mathbf{R})\frac{\partial}{\partial h}[\Theta(|\mathbf{R}-(2R_b+h)\mathbf{e}_z|-(R_b+R_s))] = \frac{1}{\beta}\int d^3R\ \delta(|\mathbf{R}|-(R_b+R_s))\frac{z}{R}n(\mathbf{R}+(2R_b+h)\mathbf{e}_z), \tag{A3}$$

where we have used Eqs. (2.1) and (2.2) and defined $n(\mathbf{R})\equiv\rho(\mathbf{R})\exp[\beta V(\mathbf{R};h)]$. In the case of a hard wall ($R_b\to\infty$) it is known that $n(\mathbf{R})$ is continuous even if the potential exhibits an infinite discontinuity. We expect the same to be true for a finite radius [44] and Eq. (2.4) then follows.

The derivation given above pertains to large and small hard spheres. It should be viewed as a special case of the relation

$$\left(\frac{\partial\Omega}{\partial h}\right)_{T,\mu,A} = -\int d^3R\ \rho[\mathbf{R}+(2R_b+h)\mathbf{e}_z]\frac{z}{R}V_2'(|\mathbf{R}|), \tag{A4}$$

which is valid for any spherically symmetric potential $V_2(|\mathbf{R}|)$ centered at $(0,0,2R_b+h)$ and acting on the fluid. The derivation of Eq. (A4) follows along the lines given above. We emphasize that in Eq. (A3) and in Eq. (A4) the potential $V_1(\mathbf{R})$, due to the obstacle 1, is arbitrary.

[1] S. Asakura and F. Oosawa, J. Chem. Phys. **22**, 1255 (1954).
[2] W. B. Russel, D. A. Saville, and W. R. Schowalter, *Colloidal Dispersions* (Cambridge University Press, Cambridge, 1989).
[3] P. Attard, J. Chem. Phys. **91**, 3083 (1989).
[4] P. Attard and G. N. Patey, J. Chem. Phys. **92**, 4970 (1990).
[5] R. Dickman, P. Attard, and V. Simonian, J. Chem. Phys. **107**, 205 (1997).
[6] Y. Mao, M. E. Cates, and H. Lekkerkerker, Physica A **222**, 10 (1995).
[7] T. Biben, P. Bladon, and D. Frenkel, J. Phys.: Condens. Matter **8**, 10 799 (1996).
[8] L. Degrève and D. Henderson, J. Chem. Phys. **100**, 1606 (1994).
[9] N. F. Carnahan and K. E. Starling, J. Chem. Phys. **51**, 635 (1969).
[10] J. R. Henderson, Mol. Phys. **59**, 89 (1986).
[11] B. Götzelmann and S. Dietrich, Phys. Rev. E **55**, 2993 (1997).
[12] J. Lyklema, *Fundamentals of Interface and Colloid Science* (Academic, London, 1991).
[13] B. Derjaguin, Kolloid-Z. **69**, 155 (1934).
[14] G. Karlström, Chem. Scr. **25**, 89 (1985).
[15] R. Kjellander and S. Sarman, Chem. Phys. Lett. **149**, 102 (1988).
[16] P. Attard, D. R. Bérard, C. P. Ursenbach, and G. N. Patey, Phys. Rev. A **44**, 8224 (1991).
[17] M. Schoen and S. Dietrich, Phys. Rev. E **56**, 499 (1997).
[18] B. Götzelmann, A. Haase, and S. Dietrich, Phys. Rev. E **53**, 3456 (1996).
[19] B. Götzelmann (unpublished).
[20] A. J. P. Nijmeijer and J. M. J. v. Leeuwen, J. Phys. A **23**, 4211 (1990).
[21] H. Reiss, H. L. Frisch, E. Helfand, and J. L. Lebowitz, J. Chem. Phys. **32**, 119 (1960).
[22] B. Baeyens and H. Verschelde, J. Math. Phys. **36**, 201 (1995).
[23] Y. Mao, M. E. Cates, and H. N. W. Lekkerkerker, Phys. Rev. Lett. **75**, 4548 (1995).
[24] J. Stecki and S. Sokołowski, Phys. Rev. A **18**, 2361 (1978).
[25] J. Stecki and S. Sokołowski, Mol. Phys. **39**, 343 (1980).
[26] S. Asakura and F. Oosawa, J. Polym. Sci. **23**, 183 (1958).
[27] Y. Mao, M. E. Cates, and H. N. W. Lekkerkerker, J. Chem. Phys. **106**, 3721 (1997).
[28] J. P. Hansen and I. R. Mc Donald, *Theory of Simple Liquids* (Academic, London, 1986).
[29] See, for example, E. Trizac, M. D. Eldridge, and P. A. Madden, Mol. Phys. **90**, 675 (1997), and references therein.
[30] J. L. Lebowitz and J. S. Rowlinson, J. Chem. Phys. **41**, 133 (1964).
[31] T. Biben and J.-P. Hansen, Phys. Rev. Lett. **66**, 2215 (1991).
[32] T. Biben and J.-P. Hansen, J. Phys.: Condens. Matter **3**, F65 (1991).
[33] H. Löwen, Physica A **235**, 129 (1997).
[34] M. Dijkstra and R. Van Roij, Phys. Rev. E **56**, 5594 (1997).
[35] M. Dijkstra and D. Frenkel, Phys. Rev. Lett. **72**, 298 (1994).
[36] A. P. Gast, C. K. Hall, and W. B. Russel, J. Colloid Interface Sci. **96**, 251 (1983).
[37] A. Vrij, Pure Appl. Chem. **48**, 471 (1976).
[38] Y. Heno and C. Regnaut, J. Chem. Phys. **95**, 9204 (1991).
[39] R. Evans and W. Schirmacher, J. Phys. C **11**, 2437 (1978).
[40] R. Evans and T. J. Sluckin, J. Phys. C **14**, 2569 (1981).
[41] Y. N. Ohshima, H. Sakagami, K. Okumoto, A. Tokoyoda, T. Igarashi, K. B. Shintaku, S. Toride, H. Sekino, K. Kabuto, and I. Nishio, Phys. Rev. Lett. **78**, 3963 (1997).
[42] P. D. Kaplan, L. P. Faucheux, and A. L. Libchaber, Phys. Rev. Lett. **73**, 2793 (1994).
[43] X. Ye, T. Narayanan, P. Tong, J. S. Huang, M. Y. Lin, B. L. Carvalho, and L. J. Fetters, Phys. Rev. E **54**, 6500 (1996).
[44] J. R. Henderson, in *Fluid Interfacial Phenomena*, edited by C. A. Croxton (Wiley, Chichester, 1986), p. 555.